Available online at www.sciencedirect.com
ScienceDirect
Journal of Catalysis 252 (2007) 69–76
JOURNAL OF CATALYSIS
www.elsevier.com/locate/jcat

Au/TiO_2 as high efficient catalyst for the selective oxidative cyclization of 1,4-butanediol to γ-butyrolactone

Jie Huang [a], Wei-Lin Dai [a,*], Hexing Li [b], Kangnian Fan [a]

[a] *Department of Chemistry and Shanghai Key Laboratory of Molecular Catalysis and Innovative Materials, Fudan University, Shanghai 200433, PR China*
[b] *Department of Chemistry, Shanghai Normal University, Shanghai 200234, PR China*

Received 3 August 2007; revised 14 September 2007; accepted 14 September 2007

Abstract

Au/TiO_2 catalysts prepared by the deposition–precipitation method showed excellent activity and selectivity in the oxidative cyclization of 1,4-butanediol to γ-butyrolactone, with high yields (>99%) under mild conditions (413 K, 1.25 MPa air). Catalysts with 3–8% gold loading and calcined at 573–673 K were all highly active for the formation of γ-butyrolactone, as demonstrated by XRD, TEM, XPS, ICP and UV–vis DRS results. It is concluded that highly dispersed small (2–10 nm) gold particles are formed with the surface enrichment of gold. The ratio of cationic gold to metallic gold depends on the treatment temperature. These findings, combined with those of the activity tests, lead to the conclusion that the surface metallic nanosized gold particles are active sites. The catalyst can be reused with no drop in activity or selectivity.

Keywords: 1,4-Butanediol; γ-Butyrolactone; Gold catalyst; Aerobic oxidation; Titania

1. Introduction

The lactones and their derivatives are widely distributed in nature [1]. The lactone ring exists in the molecules of many bioactive substances [2] and metabolic intermediates [3]. Lactones also can be used for synthesizing a variety of polymers [4–6]. Although oxidation of alcohols has been widely used for the synthesis of various chemicals, the oxidation of diols to lactones usually requires fierce reaction conditions and specific oxidants. The reaction can occur under mild conditions only in the presence of organic cooxidants, such as toluene, PhBr [7], α,β-unsaturated ketone [8,9], allyl methyl carbonate, *N*-methylmorpholine *N*-oxide, or acetone. To date, there are few reports on the catalytic oxidation of diols to lactones using molecular oxygen or air as the green oxidant, and high conversion and selectivity can be achieved only using a well-designed catalyst. Among the diol oxidations to lactones, the oxidation of 1,4-butanediol to γ-butyrolactone can be considered a typical probe reaction, because γ-butyrolactone is widely used in agriculture, the petroleum industry, pharmaceutics, and resins and fibers as an important solvent, extraction agent, and intermediate for preparing various medicines, fibers, and pesticides. The aerobic oxidation of 1,4-butanediol is an effective green approach to the synthesis of γ-butyrolactone, owing to the absence of waste or pollutant.

Although heterogeneous catalysts are widely used in manufacturing γ-butyrolactone from 1,4-butanediol via dehydrogenation processes, few studies of heterogeneous catalyst-based oxidative process have been reported, and those that exist are focused mainly on copper-based catalysts, such as Cu–Zn–Zr–Al–O [10], Cu/Cr with metal oxide as additives [11,12], and Cu/SiO_2–CaO [13]. These copper catalysts usually require high reaction temperatures, which inevitably induces side reactions. The chromium is essential to achieving satisfactory conversion, which adds to the environmental problems. Moreover, the nonoxidative process is not eco-friendly and consumes a significant amount of energy.

Nanosized gold has been widely studied recently, and it is considered an excellent catalyst in both gas- and liquid-phase oxidation [14–16], the water–gas shift reaction [17], hydrogenation, NO_x reduction [18] and other processes. Most studies

* Corresponding author. Fax: +86 21 65642978.
E-mail address: wldai@fudan.edu.cn (W.-L. Dai).

0021-9517/$ – see front matter
doi:10.1016/j.jcat.2007.09.011

are focused on gas-phase oxidation, such as CO oxidation, hydrocarbon combustion, and other selective oxidations. There has been recent interest in liquid-phase selective oxidation of α,β-diols or glycerol, including benzyl alcohol [19], polyols [20,21], and sugars [22]. Although ester can be obtained from the oxidation of primary alcohols [23], the direct oxidation of α,ω-diols (e.g., 1,4- or 1,5-diols) to form lactones on gold-based catalysts has not been reported to date.

It remains unclear how the particle size, the oxidation state of gold, the metal–support interaction, and the preparation conditions affect the activity of gold-based catalysts [24,25], although the mechanisms and the active sites of gold catalysts have been well documented [26,27]. Gold supported on different crystal phases shows difference in stability and activity [28]. The addition of metal oxide to the supported gold catalysts also may improve its catalytic performance [29–31]. The differences in preparation parameters may significantly affect gold particle size, surface properties, gold–support interaction, and electronic state, leading to the different catalytic behaviors.

In the present work, Au/TiO_2 catalysts with different gold loadings were prepared by the deposition–precipitation method and treated at various temperatures. The catalysts exhibited 99% conversion and 99% selectivity to γ-butyrolactone during liquid-phase 1,4-butanediol oxidation by air. The correlation between catalyst structural properties and catalytic performance is briefly discussed based on detailed characterizations.

2. Experimental

2.1. Catalyst preparation

Au/TiO_2 catalysts were synthesized by homogeneous deposition–precipitation. $HAuCl_4{\cdot}3H_2O$ was dissolved in 50 mL of deionized water. Urea was used as precipitation agent, with a gold/urea molar ratio of 1/200. Then 1.0 g TiO_2 (commercial Degussa P25) was added. The mixture was stirred for 2 h at 353 K, during which the pH value gradually increased from 3 to 8. The as-received precipitate was collected by filtration, washed three times with deionized water, and dried in air overnight at 373 K, followed by calcining in air for 4 h at the desired temperatures. For recycling test, the used catalyst was washed with ethanol three times to remove the contaminants, then calcined at 573 K in a muffle oven for 4 h.

2.2. Catalyst characterization

The XRD patterns were recorded on a Bruker D8 advance spectrometer with Cu$K\alpha$ radiation ($\lambda = 0.154$ nm), operated at 40 mA and 40 kV. The XPS spectra were recorded under vacuum ($<10^{-6}$ Pa) and at a pass energy of 93.90 eV on a Perkin-Elmer PHI 5000C ESCA system equipped with a dual X-ray source using an Al$K\alpha$ (1486.6 eV) anode and a hemispheric energy analyzer. All binding energies were calibrated using contaminant carbon (C 1s = 284.6 eV) as a reference. TEM micrographs were obtained on a JOEL JEM 2010 transmission electron microscope. The UV–vis DRS spectra were collected using a Shimadzu UV-2450 spectrophotometer from 200 to 800 nm using $BaSO_4$ as background. The gold loadings were determined by the inductively coupled plasma (ICP, thermo E.IRIS).

2.3. Activity test

The activity tests were carried out at 393 (or 413) K in an autoclave equipped with a magnetic stirrer. In a typical run of reactions, 1.4 g of 1,4-butanediol was dissolved in 20 mL of tributyl phosphate (TBP), followed by the addition of a specified amount of Au/TiO_2 catalyst according to a gold:1,4-butanediol molar ratio of 1:200. Then 1.25 MPa air was filled, and the reaction was initiated by vigorous stirring. The reaction mixture was sampled at regular time intervals for product analysis by both GC and GC-MS to determine the conversion and selectivities.

3. Results

3.1. X-ray diffraction analyses

Figs. 1 and 2 show the XRD patterns of Au/TiO_2 catalysts with different loadings calcined at various temperatures. The XRD patterns display diffraction peaks indicative of both rutile and anatase phases in Degussa P25, implying the support was stable during the precipitation of gold and calcination even at 773 K. The diffraction peak at $2\theta = 77.4°$ characteristic of Au(311) was chosen to investigate the crystalline properties of gold, because the peak at $2\theta = 64.4°$ indicative of Au(220) was overlapped by the peak corresponding to rutile(310) at $2\theta = 64.0°$. No signals representing the gold species were observed for Au/TiO_2 catalysts after calcination at below 573 K, which can be attributed to the high dispersion of gold particles

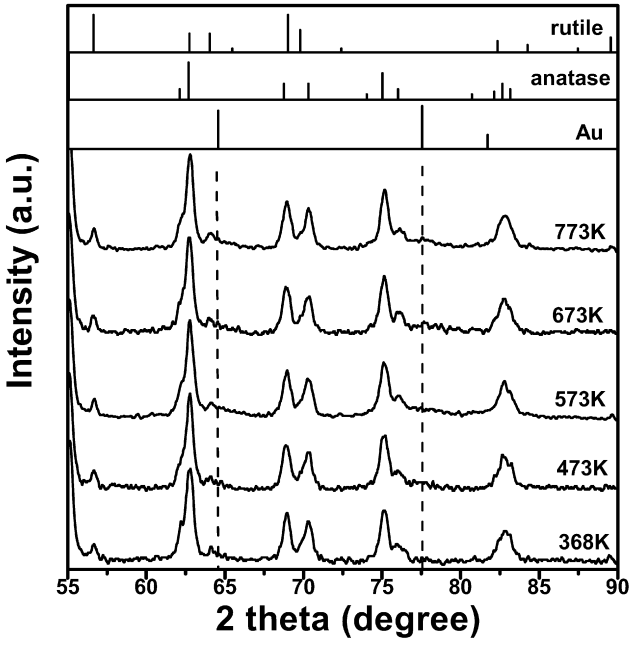

Fig. 1. XRD patterns of Au/TiO_2 catalysts calcined at 773, 673, 573, and 473 K, and dried at 368 K.

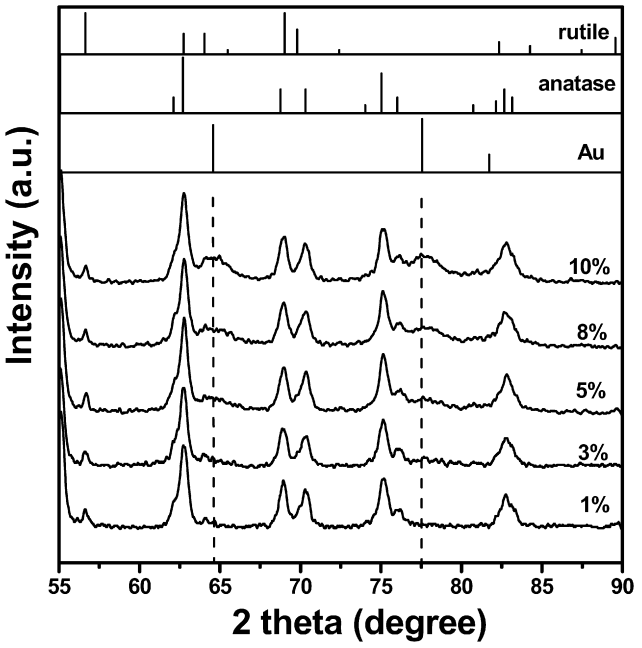

Fig. 2. XRD patterns of Au/TiO_2 catalysts with 1, 3, 5, 8, and 10% loadings.

on the TiO_2 support. Further increases in calcination temperature result in the agglomeration of gold particles, corresponding to the gradual appearance of the diffraction peak at $2\theta = 77.4°$.

At very low gold loading (<3%), no significant signals indicative of Au species were observed owing to the high dispersion. The gold peaks became sharper and more obvious with the rise in gold loading, and even the peak corresponding to Au(220) at $2\theta = 64.4°$ can be well resolved when the gold loading reaches 10%. The increased intensity of the Au(311) peak may be caused by increases in the amount of gold or the growth of gold particles. However, combined with the TEM morphologies (as discussed below), the increase in gold loading from 3 to 8% has little or no significant influence on the gold particle size, but further increases in gold loading lead to an abrupt increase in gold particle size.

3.2. TEM results

The TEM images in Fig. 3 show the TiO_2 particle size range in 15–30 nm and the gold particle size in the range of 1–10 nm for all of the as-prepared Au/TiO_2 catalysts. The HRTEM image displays spherical gold particles. Raft-like gold particles were also observed but are not shown here. As reported previously [32–34], each gold particle exposes its (111) plane to contact with the TiO_2 surface. More than 100 such particles were counted in TEM images to calculate the average sizes of these catalysts, as given in Tables 1 and 2. The differences in synthesis conditions and loadings affect the particle size distribution. The smallest gold particles were observed in the Au/TiO_2 catalyst with 3% gold loading and calcined at 573 K, as further confirmed by the gold distribution histogram in Fig. 4. The higher calcination temperature led to enhanced particle size, obviously due to the congregation of gold particles. The sample calcined at 473 K exhibited a larger particle size (5.6 nm in average), possibly due to the incomplete reduction, as supported by the subsequent XPS and UV–vis DRS characterizations.

Table 1
The physico-chemical properties and catalytic activity of 3% Au/TiO_2 catalysts calcined at different temperatures

Calcined temperature (K)	d_{Au} (nm)[a]	Au_{surf} (%)[b]	Au(0) (%)[c]	Au(III) (%)[c]	Yield (%)[d]	Reaction rate (mol/(mol h))[e]	Specific rate (mmol/(m^2 h))[f]
RT	–	20	49	51	0	0	–
368	–	10	68	32	2	0.5	–
473	5.6	6.4	82	18	54	17.9	1.6
573	4.5	7.1	100	0	74	21.7	1.6
673	5.4	5.9	100	0	66	20.7	1.8
773	–	5.2	100	0	47	18.3	–

[a] Gold particle size was calculated by counting more than 100 particles from the TEM images.
[b] The surface gold loading, Au_{surf}% was calculated by the surface Au to Ti atomic ratio obtained from the XPS spectra.
[c] The metallic and cationic gold content was obtained from the peak area of Au(0) and Au(III) species from the XPS data.
[d] The yield is obtained at 393 K after 8 h reaction.
[e] The amount of 1,4-butanediol reacted per mol gold per hour.
[f] mmol of reacted 1,4-butanediol per m^2 active gold per hour.

Table 2
The physico-chemical properties and catalytic activity of Au/TiO_2 catalysts with different loadings

Gold loading (%)	Au content (wt%)	Au_{surf} (%)[a]	d_{Au} (nm)[b]	Yield (%)[c]	Reaction rate (mol/(mol h))[d]	Specific rate (mmol/(m^2 h))[e]
1	0.9	2.7	–	47	21.3	–
3	2.6	5.9	5.4	59	21.4	1.8
5	4.2	12	–	60	20.4	–
8	6.4	21	5.0	65	24.3	2.0
10	8	22	6.2	44	18.6	1.9

[a] The surface gold loading, Au_{surf}% was calculated by the surface Au to Ti atomic ratio obtained from the XPS spectra.
[b] Gold particle size was calculated by counting more than 100 particles from the TEM images.
[c] The yield is obtained at 393 K after 9 h reaction.
[d] The amount of 1,4-butanediol reacted per mol gold per hour.
[e] mmol of reacted 1,4-butanediol per m^2 active gold per hour.

Note that many particles smaller than 4.0 nm were observed in the Au/TiO_2 catalyst with 8% gold loading, although the average particle size was larger than that in the Au/TiO_2 catalyst with 3% gold loading. This indicates a nonuniform distribution of the gold particles, because the gold particles more easily congregated or formed multiple conjunctions with the support at high gold loadings.

3.3. XPS

The XPS spectra of the Au/TiO_2 catalysts calcined at different temperatures are shown in Fig. 5, and the surface gold contents calculated based on XPS spectra are listed in Tables 1 and 2. These findings demonstrate the presence of the nonoxidized gold species corresponding to a binding energy of 83.7 eV at the Au $4f_{7/2}$ level and the surface enrichment of gold species. A slightly negative shift in comparison with bulk gold

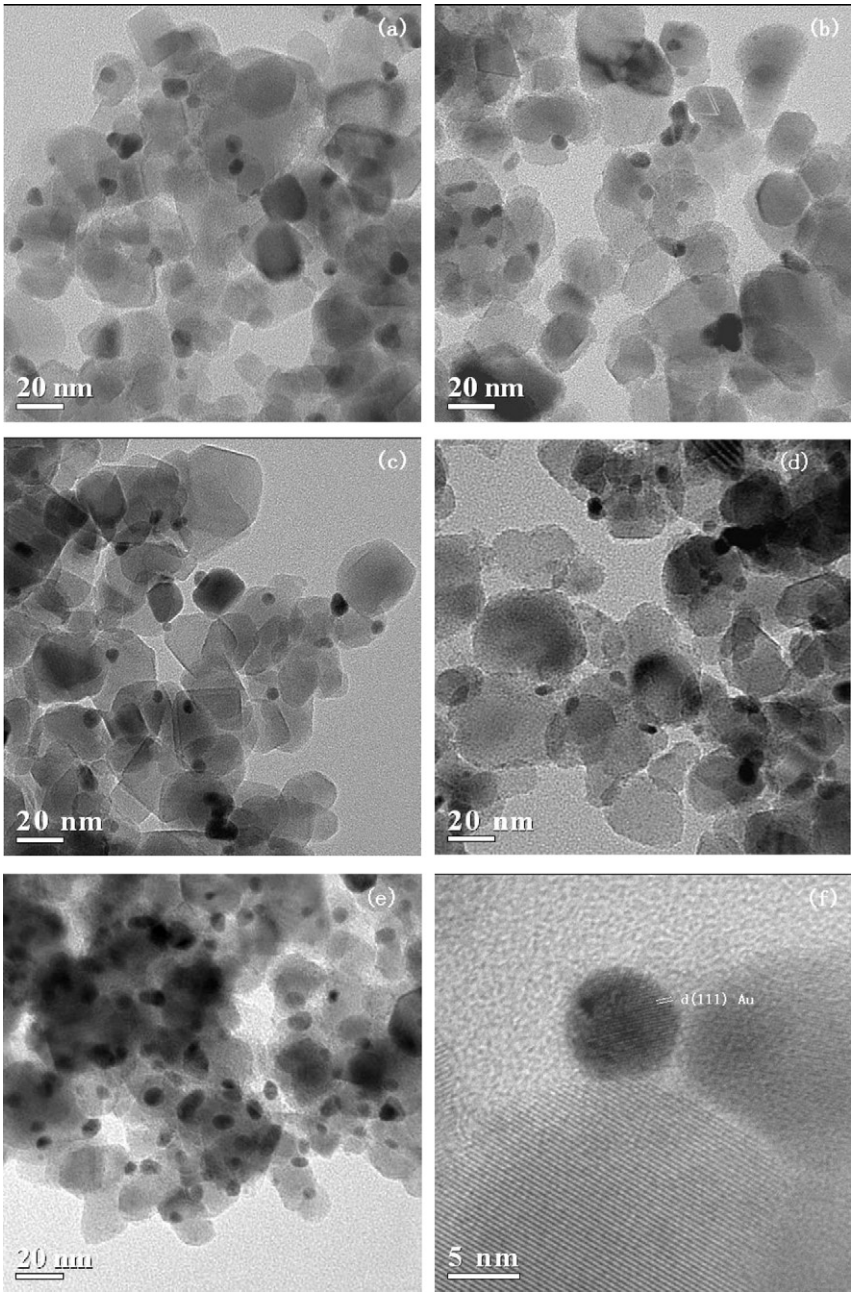

Fig. 3. TEM image of Au/TiO_2 catalysts. (a) 3% Au/TiO_2 calcined at 673 K; (b) 3% Au/TiO_2 calcined at 573 K; (c) 3% Au/TiO_2 calcined at 473 K; (d) 8% Au/TiO_2 calcined at 673 K; (e) 10% Au/TiO_2 calcined at 673 K; (f) HRTEM image of 3% Au/TiO_2 calcined at 573 K.

(normally at 84.0 eV) suggests the formation of a strong metal–support interaction.

The XPS spectra of the catalysts dried at room temperature and 368 K showed two peaks at 85.1 and 83.7 eV, which can be assigned to the Au(III) and Au(0) species, respectively, indicating the presence of positively charged gold. It is commonly believed that the cationic gold species cannot be completely reduced below 573 K [35,36]. The XPS spectra demonstrate the existence of Au^{3+} in the catalysts calcined at temperatures below 573 K, which can be further confirmed by observing color changes of the samples. The catalyst dried at room temperature had a light-yellow color indicative of the Au(III) species, turning lighter after calcination at 368 K due to the reduction of Au(III). Table 1 shows that the Au/TiO_2 catalysts dried at room temperature and calcined at 368 K contained 51 and 32% Au(III) species, respectively. Calcination at temperatures above 473 K induced a dark-purple color characteristic of nanosized metallic gold. The surface gold enrichment is most likely due to the nonreduction of cationic gold species. During the synthesis process, gold is deposited on the surface of the support in the form of $Au(OH)_3$. The subsequent washing procedure had no influence on the $Au(OH)_3$ species, but simply removed urea and chloride cations. These $Au(OH)_3$ species were mainly adsorbed on the outer surface of the support due to the weak interaction with the support, leading to the surface-enriched gold species. Calcination at high temperature resulted in the

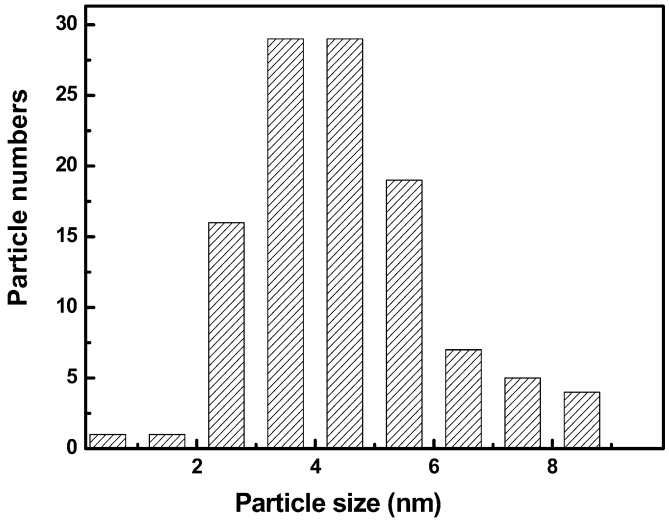

Fig. 4. Particle size distribution of the 3% Au/TiO_2 catalyst calcined at 573 K.

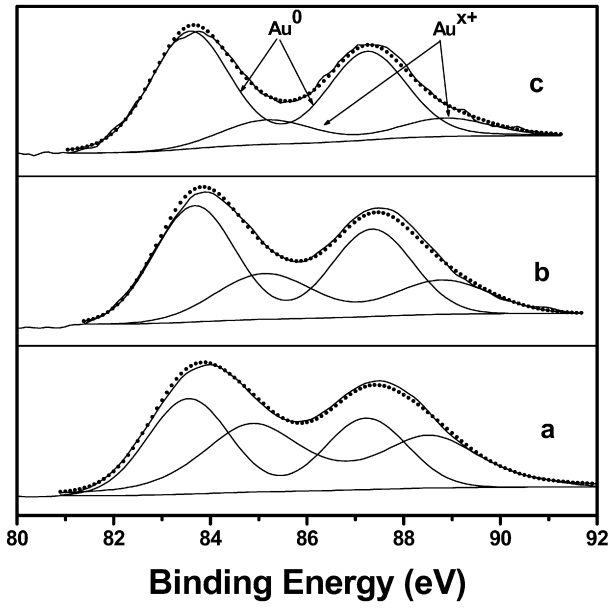

Fig. 5. XPS spectra of 3% Au/TiO_2 catalysts treated at (a) room temperature; (b) 368 K and (c) 473 K.

reduction of oxidized gold to metallic gold and also induced a strong metal–support interaction. As a result, gold species tended to enter the internal surface of the support, leading to a decreased surface enrichment of gold species. Moreover, the strong metal–support interaction may have influenced the electronic properties of the surface gold, possibly accounting for the negative shift in binding energy of the surface gold compared with the bulk gold.

It is not surprising to find that the surface gold content increased steadily with the increment of gold loading up to 8%. The surface gold content is known to be always greater than the bulk gold content in the supported Au catalyst and to reach a maximum value at a certain gold loading because of the surface saturation. Based on XPS and ICP analysis, the Au/Ti atomic ratio, the surface Au/TiO_2 ratio (wt%), and the gold loading

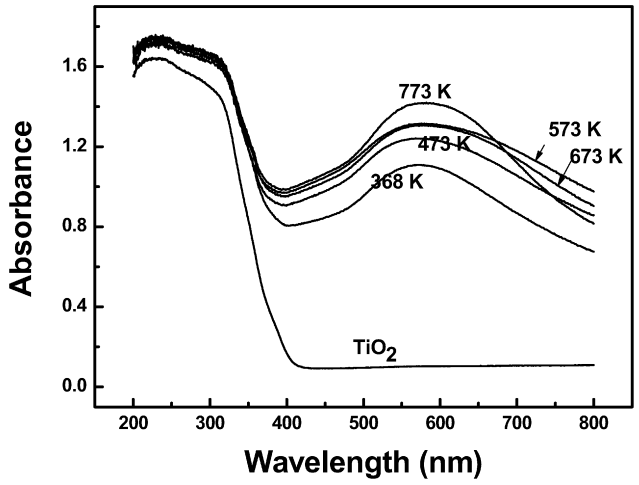

Fig. 6. UV–vis DRS spectra of 3% Au/TiO_2 calcined at 473, 573, 673, and 773 K, and dried at 368 K.

were determined; these values are given in Table 2. Clearly, the surface gold content at 10% gold loading is only slightly greater than that at 8% gold loading, suggesting the Au/TiO_2 catalyst reached surface saturation at 8% gold loading. In such a surface-saturated Au/TiO_2 catalyst, gold particles were closely packed and could congregate easily, leading to increased particle size, as confirmed by XRD patterns and TEM images.

3.4. UV–vis DRS

Fig. 6 shows UV–vis DRS spectra of the catalysts treated at different temperatures. The absorption around 570 nm is due to the metallic nanosized gold particle plasma resonance, which usually appears when the wavelength of the light exceeds the particle size [33]. The absorbance from 200 to 350 nm resulted from the P25 support. The appearance of the plasmon band at around 570 nm suggests that the metallic gold was already partially formed after being treated at 368 K. A stronger peak was observed in the sample calcined at 473 K. The intensities of the other catalysts were almost the same, and it can be assumed that gold was not completely reduced at calcination temperatures below 473 K, well consistent with the XPS results.

3.5. 1,4-Butanediol oxidation activity

It was surprising to find that all the catalysts with gold loading of 3–8% calcined at 573–673 K exhibited excellent catalytic performance during reaction at 413 K. Both conversion and selectivity were >99%, and the TOF value of the Au/TiO_2 catalyst with 3% gold loading calcined at 573 K was 64 h^{-1}, demonstrating good potential for industrial applications based on the following considerations: (1) the extremely high yield of γ-butyrolactone significantly decreases the cost of the raw material; (2) the byproduct of very low content can be easily separated by distillation owing to its high boiling point, which can ensure the high purity of the target product γ-butyrolactone; (3) the heterogeneous catalyst can be conveniently separated from the reaction system by simple filtration, which can ensure

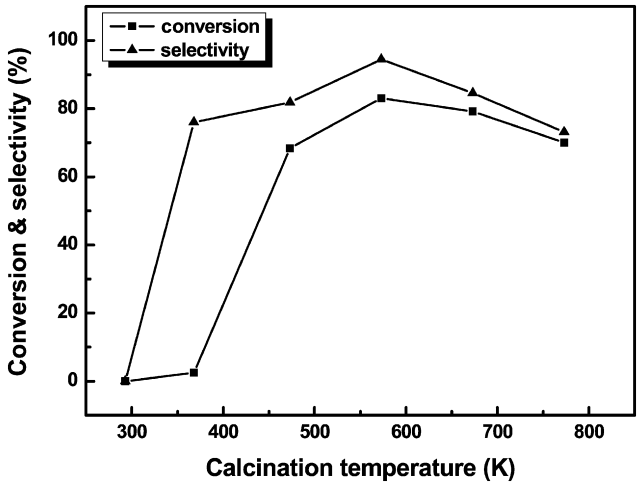

Fig. 7. Dependence of calcination temperature of 3% Au/TiO_2 catalyst and 1,4-butanediol conversion and γ-butyrolactone selectivity at 393 K for 9 h.

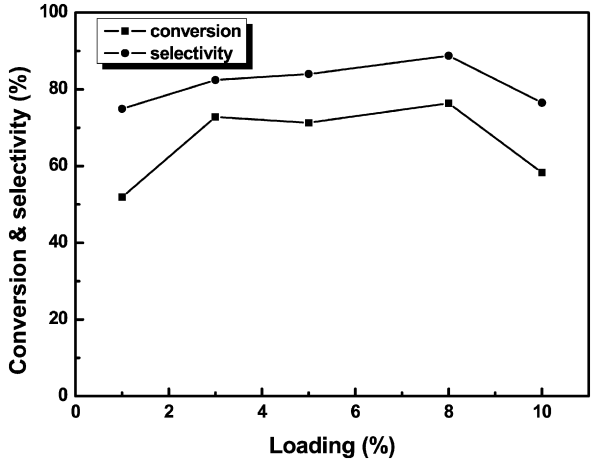

Fig. 8. Dependence of gold loadings of Au/TiO_2 catalysts calcined at 673 K and 1,4-butanediol conversion and γ-butyrolactone selectivity. Reaction was carried out at 393 K for 8 h.

the recycling use and also diminish the environmental pollution from heavy metallic ions; (4) the reaction temperature is much lower than the direct dehydrogenation process over copper-based catalysts (513 K), and no extra energy is needed, because the reaction itself is strongly exothermic.

The catalytic performance was also examined during reaction at 393 K to demonstrate the slight affect of calcination temperature and gold loading. The results are summarized in Tables 1 and 2 and also shown in Figs. 7 and 8. The Au/TiO_2 catalyst with 8% gold loading calcined at 573 K showed the greatest activity. The catalyst dried at room temperature was inactive at all temperatures. The activity increased with increasing calcination temperature owing to the reduction of gold ions. However, a very high calcination temperature (773 K) diminished activity, possibly due to the severe agglomeration of gold particles. Because the selectivity versus calcination temperature plot shows a typical volcano shape with the highest value obtained at 573 K (Fig. 7), 573 K is determined to be the optimum calcination temperature for achieving the highest γ-butyrolactone yield.

Using the Au/TiO_2 catalyst calcined at 673 K, the reaction conversion fluctuated around 71–76% when the gold loading was varied from 3 to 8%, and then decreased abruptly to 58% at 10% gold loading. The selectivity also increased slightly with the increment of gold loading from 3 to 8%, and then decreased when the gold loading exceeded 10%.

The nature of active sites in gold catalysts remains controversial. Some researchers claim that the existence of gold cations contributes to the high activity [37,38], whereas others insist that anionic gold ($Au^{\delta-}$) is formed due to the electron transfer from the oxide support to gold [39,40]. Moreover, Overbury et al. [41] even suggested that the low-coordinated sites, edge and corner sites, interfacial perimeter, and hemispherical gold clusters were the active species [24]. Moreover, it also has been reported that the particle size and crystal phase of the support were the crucial parameters at gold particle size of ca. 4–6 nm [42]. Based on the activity test on the Au/TiO_2 catalysts dried at room temperature and calcined at 368 K, we conclude that the oxidized gold was inactive for 1,4-butanediol oxidation. Activity increased with increasing calcination temperature due to the enhanced degree of reduction. The Au/TiO_2 catalyst calcined at 673 K exhibited lower activity due to the significant gathering of gold particles. The Au/TiO_2 catalyst calcined at 673 K exhibited lower activity at a gold loading of 10%, which also could be attributed to the agglomeration of gold particles, taking into account that the degree of reduction of the catalyst already reached a maximum value at a calcination temperature of 673 K.

In addition, the surface gold content also plays an important role in determining the activity. As discussed above, the Au/TiO_2 catalyst is surface-enriched with gold species, which may be beneficial for heat transference [43] and the formation of multiple contact with the support. Such multiple contact can increase the gold–metal oxide contact boundaries and also generate some gold–support junctions that are favorable for the reactions, leading to enhanced activity [42]. Because the Au/TiO_2 had already reached surface saturation at 8% gold loading, any further increase in the gold loading could only induce particle agglomeration, leading to the reduced activity.

4. Discussion

For different reactions, the gold catalysts displayed both structural sensitivity and structural insensitivity. To investigate whether or not the reaction is structurally sensitive, the influence of the surface gold content should be excluded, because a smaller particle size results in a larger gold surface area, corresponding to greater activity. This means that the greater activity obtained at smaller gold particle size is due solely to the increased surface gold content. Therefore, we calculated the reaction rate per unit gold surface area with the aim of investigating the relation between the activity and the particle size. Considering the approximation in the calculation of the gold surface area, including assuming the gold particle as sphere, and the use of average diameter, the reaction rate per unit gold surface area of all the catalysts with different particle sizes can be considered in the same order. From the findings given in Tables 1

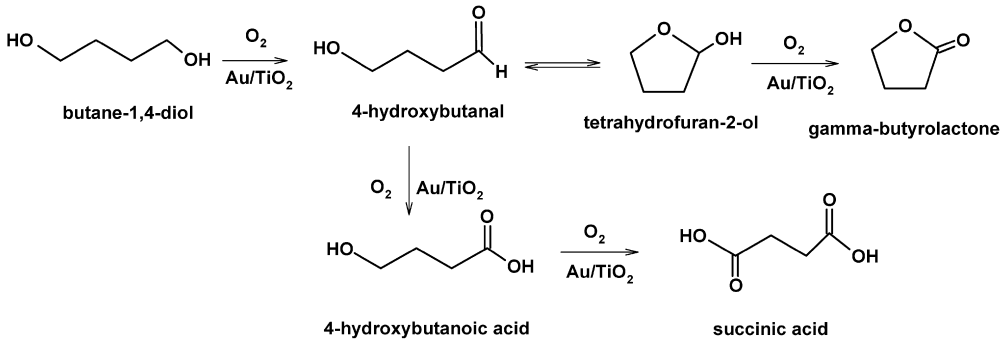

Scheme 1. Proposed reaction route for the aerobic oxidation of 1,4-butanediol.

Table 3
Reusability of 3% Au/TiO_2 calcined at 573 K[a]

Run	Conversion (%)	Selectivity (%)	Yield (%)
Fresh	99	100	99
1	97	96	93
2	99	100	99

[a] Reaction conditions: 0.5 g 3% Au/P25, 0.7 g 1,4-butanediol, 20 mL TBP, 1.25 MPa air, 413 K, 8 h.

and 2, we can readily conclude that the oxidative cyclization of 1,4-butanediol to γ-butyrolactone is not a structurally sensitive reaction.

No significant byproducts were detected by GC, even though the selectivity was <100% during the reaction at 393 K. We believe that as the selectivity increased with increasing reaction time, at least one intermediates with a high boiling point, such as tetrahydrofuran-2-ol, was formed during the reaction (see Scheme 1) [44,45]. First, 1,4-butanediol was oxidized to 4-hydroxybutanal, along with the formation of inner molecular hemiacetal, tetrahydrofuran-2-ol. Then the tetrahydro-2H-pyran-2-ol was dehydrogenated to the target product γ-butyrolactone. Possible side reactions were further oxidation to 4-hydroxybutanoic acid and succinic acid. However, the formation of acids or other byproducts could not be detected during reactions at 413 or 393 K, obviously owing to the higher selectivity of the as-prepared Au/TiO_2 catalyst.

Even though the highest yield was achieved on the Au/TiO_2 catalyst with 8% gold loading, the Au/TiO_2 catalyst with 3% gold loading was chosen as a candidate for potential industrial applications, based on cost considerations. The durability of the Au/TiO_2 catalyst with 3% gold loading was examined through recycling tests. As shown in Table 3, the present Au/TiO_2 catalyst did not deactivate during the reaction course. In addition, no leaching of gold was detected in the reaction mixture and no change of the particle size of gold was seen, demonstrating the catalyst's good potential in industrial applications.

5. Conclusion

A series of Au/TiO_2 catalysts with well-dispersed nanosized gold particles on the support surface were synthesized using a homogeneous deposition–precipitation method that showed good activity and selectivity during liquid-phase aerobic oxidation of 1,4-butanediol to γ-butyrolactone under mild conditions. Both calcination temperature and gold content had a significant affect on catalytic performance. The greatest 1,4-butanediol conversion and γ-butyrolactone yield were obtained on the catalyst with 8% gold loading and calcined at 573–673 K, due to the small gold particle size and absolute degree of reduction, taking into account that the metallic gold was the active site. The effect of the gold loading on the catalytic behavior also could be attributed to the surface enrichment of gold species, and Au/TiO_2 catalyst reached surface saturation at 8% gold loading, favoring the dispersion of gold particles and also facilitating heat transfer. Loadings of 3–8% are all acceptable values, not so high as to lead to the congregation of gold or too low so as to form the gold–support junctions that are beneficial to the title reaction. The Au/TiO_2 catalyst was quite stable and could be used repetitively without significant deactivation.

Acknowledgments

This work was supported by the Major State Basic Resource Development Program (grant 2003CB615807), the National Science Foundation of China (projects 20407006 and 20573024), and the Natural Science Foundation of Shanghai Science & Technology Committee (project 06JC14004).

References

[1] M. Kataoka, K. Honda, K. Sakamoto, S. Shimizu, Appl. Microbiol. Biotechnol. 75 (2007) 257.
[2] J.T. Isaacs, BJU Int. 96 (2005) 35.
[3] J. Alary, Y. Fernandez, L. Debrauwer, E. Perdu, F. Gueraud, Chem. Res. Toxicol. 16 (2003) 320.
[4] A.C. Albertsson, I.K. Varma, Biomacromolecules 4 (2003) 1466.
[5] H. Lee, F. Zeng, M. Dunne, C. Allen, Biomacromolecules 6 (2005) 3119.
[6] K. Shiro, Macromol. Symp. 240 (2006) 178.
[7] Y. Tamaru, Y. Yamada, K. Inoue, Y. Yamamoto, Z. Yoshida, J. Org. Chem. 48 (1983) 1286.
[8] Y. Ishii, K. Suzuki, T. Ikariya, M. Saburi, S. Yoshikawa, J. Org. Chem. 51 (1986) 2822.
[9] Y. Ishii, K. Osakada, T. Ikariya, M. Saburi, S. Yoshikawa, J. Org. Chem. 51 (1986) 2034.
[10] N. Ichikawa, S. Sato, R. Takahashi, T. Sodesawa, K. Inui, J. Mol. Catal. A Chem. 212 (2004) 197.
[11] T. Ichiki, K. Mori, S. Suzuki, H. Ueno, K. Kobayashi, US patent 5210229 (1993), Tonen Chemical Corporation.
[12] R. Sigg, R. Hans, US patent 5426195 (1995), Huels Aktiengesellschaft.

[13] M.H. Jochen, F.F. Pape, J. Simon, A. Henne, M. Hesse, U. Kohler, R. Dostalek, C.F. Erdbrugger, D. Kratz, US patent 6093677 (2000), BASF Aktiengesellschaft.
[14] G.C. Bond, C. Louis, D.T. Thompson, Catalysis by Gold, Imperial College Press, London, 2006, p. 217.
[15] D.Y. Cha, G. Parravano, J. Catal. 18 (1970) 200.
[16] L. Guczi, G. Peto, A. Beck, K. Frey, O. Geszti, G. Molnar, C. Daroczi, J. Am. Chem. Soc. 125 (2003) 4332.
[17] V. Idakiev, T. Tabakova, A. Naydenov, Z.Y. Yuan, B.L. Su, Appl. Catal. B Environ. 63 (2006) 178.
[18] A. Ueda, M. Haruta, Appl. Catal. B Environ. 18 (1998) 115.
[19] V.R. Choudhary, A. Dhar, P. Jana, R. Jha, B.S. Uphade, Green Chem. 7 (2005) 768.
[20] L. Prati, M. Rossi, J. Catal. 176 (1998) 552.
[21] L. Prati, F. Porta, Appl. Catal. A Gen. 291 (2005) 199.
[22] M. Comotti, C.D. Pina, R. Matarrese, M. Rossi, A. Siani, Appl. Catal. A Gen. 291 (2005) 204.
[23] D.I. Enache, D.W. Knight, G.J. Hutchings, Catal. Lett. 103 (2005) 43.
[24] G. Bamwenda, S. Tsubota, T. Nakamura, M. Haruta, Catal. Lett. 44 (1997) 83.
[25] N. Dimitratos, A. Villa, C.L. Bianchi, L. Prati, M. Makkee, Appl. Catal. A Gen. 311 (2006) 185.
[26] Z.P. Liu, P. Hu, A. Alavi, J. Am. Chem. Soc. 124 (2002) 14770.
[27] D. Tibiletti, A. Amieiro-Fonseca, R. Burch, Y. Chen, M. Fisher, A. Goguet, C. Hardacre, P. Hu, D. Thompsett, J. Phys. Chem. B 109 (2005) 22553.
[28] W. Yan, B. Chen, S.M. Mahurin, V. Schwartz, D.R. Mullins, A.R. Lupini, S.J. Pennycook, S. Dai, S.H. Overbury, J. Phys. Chem. B 109 (2005) 10676.
[29] A.C. Gluhoi, N. Bogdanchikova, B.E. Nieuwenhuys, J. Catal. 229 (2005) 154.
[30] W. Yan, S.M. Mahurin, Z. Pan, S.H. Overbury, S. Dai, J. Am. Chem. Soc. 127 (2005) 10480.
[31] F. Moreau, G.C. Bond, Catal. Today 114 (2006) 362.
[32] T. Akita, K. Tanaka, S. Tsubota, M. Haruta, J. Electron Microsc. 49 (2000) 657.
[33] R. Zanella, S. Giorgio, C.H. Shin, C.R. Henry, C. Louis, J. Catal. 222 (2004) 357.
[34] M. Haruta, Cattech 6 (2002) 102.
[35] F. Boccuzzi, A. Chiorino, M. Manzoli, P. Lu, T. Akita, S. Ichikawa, M. Haruta, J. Catal. 202 (2001) 256.
[36] M. Date, Y. Ichihashi, T. Yamashita, A. Chiorino, F. Boccuzzi, M. Haruta, Catal. Today 72 (2002) 89.
[37] J. Guzman, B.C. Gates, J. Am. Chem. Soc. 126 (2004) 2672.
[38] L. Fu, N.Q. Wu, J.H. Yang, F. Qu, D.L. Johnson, M.C. Kung, H.H. Kung, V.P. Dravid, J. Phys. Chem. B 109 (2005) 3704.
[39] B. Yoon, H. Häkkinen, U. Landman, A.S. Wörz, J.M. Antonietti, S. Abbet, K. Judai, U. Heiz, Science 307 (2005) 403.
[40] L.M. Molina, B. Hammer, Phys. Rev. B 69 (2004) 155424.
[41] S.H. Overbury, V. Schwartz, D.R. Mullins, W. Yan, S. Dai, J. Catal. 241 (2006) 56.
[42] X. Zhang, H. Wang, B.Q. Xu, J. Phys. Chem. B 109 (2005) 9678.
[43] N.R.E. Radwan, E.A. El-Sharkawy, A.M. Youssef, Appl. Catal. A Gen. 281 (2005) 93.
[44] A. Abad, P. Concepción, A. Corma, H. García, Angew. Chem. Int. Ed. 44 (2005) 4066.
[45] Z.G. Tian, W.W. Hu, S.L. Lu, J. Xiangfan Univ. 24 (2003) 42.